Objective-first design of high-efficiency, small-footprint couplers between arbitrary nanophotonic waveguide modes

Jesse Lu* **and Jelena Vučković**
Stanford University, Stanford, California, USA.
jesselu@stanford.edu

Abstract: We present an algorithm for designing high efficiency (∼98%), small-footprint (1.5-4 square vacuum wavelengths) couplers between arbitrary nanophotonic waveguide modes in two dimensions. Our "objective-first" method is computationally fast (15 minutes on a single-core personal computer), requires no trial-and-error, and does not require guessing a good starting design. We demonstrate designs for various coupling problems which suggest that our method allows for the design of any single-mode, linear optical device.

OCIS codes: (230.7370) Waveguides; (130.3990) Micro-optical devices.

References and links

1. Y. Tang, Z. Wang, L. Wosinski, U. Westergren, and S. He, "Highly efficient nonuniform grating coupler for silicon-on-insulator nanophotonic circuits," Opt. Lett. **35**, 1290–1292 (2010).
2. K. K. Lee, D. R. Lim, L.C. Kimerling, J. Shin, and F. Cerrina, "Fabrication of ultralow-loss Si/SiO2 waveguides by roughness reduction," Opt. Lett. **26**, 1888–1890 (2001).
3. Y. A. Vlasov, M. O'Boyle, H. F. Hamann, and S. J. McNab, "Active control of slow light on a chip with photonic crystal waveguides," Nature **438**, 65–69 (2005).
4. M. Lipson, "Guiding, modulating, and emitting light on silicon-challenges and opportunities," J. Lightwave Technol. **23**, 4222–4238 (2005).
5. J. Van Campenhout, P. Rojo Romeo, P. Regreny, C. Seassal, D. Van Thourhout, S. Verstuyft, L. Di Cioccio, J.-M. Fedeli, C. Lagahe, and R. Baets, "Electrically pumped InP-based microdisk lasers integrated with a nanophotonic silicon-on-insulator waveguide circuit," Opt. Express **15**, 6744–6749 (2007).
6. L. Tang, S. E. Kocabas, S. Latif, A. K. Okyay, D. S. Ly-Gagnon, K. C. Saraswat, and D. A. B. Miller, "Nanometre-scale germanium photodetector enhanced by a near-infrared dipole antenna," Nat. Photonics **2**, 226–229 (2008).
7. J. Lu, S. Boyd, and J. Vuckovic, "Inverse design of a three-dimensional nanophotonic resonator," Opt. Express **19**, 10563-10750 (2011).
8. G. Veronis, and S. Fan, "Theoretical investigations of compact couplers between dielectric slab waveguides and two-dimensional metal-dielectric-metal plasmonic waveguides," Opt. Express **15**, 1211-1221 (2007).
9. R. Yang, R. A. Wahsheh, Z. Lu, and M. A. G. Abushagur, "Efficient light coupling between dielectric slot waveguide and plasmonic slot waveguide," Opt. Lett. **35**, 649-651 (2010).
10. `www.github.com/JesseLu/objective-first`

1. Motivation

Optical mode conversion, the efficient transfer of photons from one guided mode to another, is a fundamental requirement in nanophotonics. For instance, efficient conversion between waveguides modes is essential for:

#161309 - $15.00 USD Received 11 Jan 2012; revised 7 Mar 2012; accepted 7 Mar 2012; published 14 Mar 2012

- Coupling to and from optical fiber [1], to communicate with the outside world.
- Coupling between various nanophotonic waveguides, since different waveguides are best suited for different applications. For example, ridge waveguides seem ideal for low-loss transport [2], but other waveguides, such as photonic crystal waveguides or slot waveguides, may be better suited for slow-light [3] or nonlinear optical devices based on localized field intensities [4].
- Coupling between different materials systems such as passive, active [5], and metallic [6] devices.

In fact, the problem of converting between nanophotonic modes is essentially the function of all linear nanophotonic devices, since any linear device is completely characterized by its input and output modes and the coupling coefficients between them.

In this paper, we present a method to solve the problem of designing single-mode, linear nanophotonic devices. We then demonstrate this method by designing coupling structures between various nanophotonic waveguides. Furthermore, we show that our method does not require a good initial design, is computationally fast, and can generate high efficiency couplers within a very small footprint.

2. Objective-first approach

Physical structures are typically designed by solving the following problem:

$$\begin{aligned} \text{decrease} \quad & f(x) && \text{(1a)} \\ \text{subject to} \quad & g(x,p) = 0, && \text{(1b)} \end{aligned}$$

where x is the field variable and p is the structure variable. Here, $f(x)$, the *design objective*, calculates the performance of the device (e.g. amount of power lost); while $g(x,p)$ is the underlying physical equation for the system (e.g. the electromagnetic wave equation).

In contrast, the objective-first approach solves

$$\begin{aligned} \text{decrease} \quad & \|g(x,p)\|^2 && \text{(2a)} \\ \text{subject to} \quad & f(x) = 0, && \text{(2b)} \end{aligned}$$

where $\|g(x,p)\|^2$ is the *physics residual*. We term this formulation "objective-first" because the design objective is prioritized even above satisfying physics; specifically, we force our design to always exhibit the desired performance ($f(x) = 0$), even at the expense of not perfectly satisfying the underlying physics which governs its operation.

The motivation behind this formulation is two-fold. First, this approach allows one to arrive at a locally-optimal design rapidly by allowing x and p to vary independently, as opposed to Eq. 1 where the value of x is completely dependent on p. Second, it enables an increase in the likelihood of arriving at a high efficiency design by forcibly imposing $f(x) = 0$, and thereby circumvents any local optima consisting of low-performance devices.

3. Objective-first design of waveguide couplers

We now demonstrate the objective-first approach by designing waveguide couplers in two-dimensions. As such, we do not analyze effects which are only present in full three-dimensional systems, such as out-of-plane losses. Specifically, we work in the two-dimensional transverse electric mode, choosing H_z as the field variable x, and ε^{-1} (the inverse of the permittivity) as the structure variable p. This results in the following form of the physics residual,

$$\|g(x,p)\|^2 = \|g(H_z,\varepsilon^{-1})\|^2 = \|\nabla \times \varepsilon^{-1} \nabla \times H_z - \mu_0 \omega^2 H_z\|^2, \tag{3}$$

#161309 - $15.00 USD Received 11 Jan 2012; revised 7 Mar 2012; accepted 7 Mar 2012; published 14 Mar 2012

where ω is the angular frequency, and μ_0 is the permeability of free-space.

In order to produce a method applicable to the design of any linear nanophotonic device, we note that its performance will be completely characterized by the fields along its boundary, and therefore, we choose a boundary-value formulation for the design objective as shown in Fig. 1. Namely, we first compute the boundary fields needed to obtain perfect performance, H_z^{perfect}, and then form the design objective as

$$f(x) = f(H_z) = \left[\begin{array}{c} H_z - H_z^{\text{perfect}} \\ \frac{\partial H_z}{\partial n} - \frac{\partial H_z^{\text{perfect}}}{\partial n} \end{array} \right]_{\text{boundary}} = 0, \tag{4}$$

where $\partial H_z / \partial n$ denotes the spatial derivative in the direction normal to the boundary.

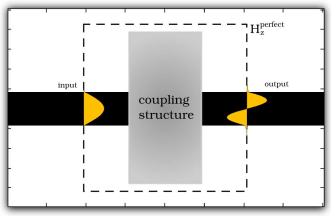

Fig. 1. Boundary-value formulation of the design objective. The values of H_z^{perfect}, defined along the dashed box surrounding the design area (coupling structure), are shown in orange. The values of H_z^{perfect} along the top and bottom edges of the dashed box are set to zero. In this schematic, the fundamental and second-order waveguide modes have been chosen as the input and output modes respectively.

Such a design objective is both extremely simple and widely adaptable to the design of linear nanophotonic devices in general. On the other hand, such a formulation often prohibits the physics residual from disappearing completely; however, we find that very good device performance is still obtained as long as the physics residual is sufficiently small.

Lastly, we employ an alternating directions strategy, where both x and p are solved iteratively [7] and limit the allowable values of ε to be between the permittivity of vacuum and of silicon,

$$\varepsilon_0 \leq \varepsilon \leq \varepsilon_{\text{silicon}}. \tag{5}$$

Note that a completely binary structure, where $\varepsilon = \{\varepsilon_0, \varepsilon_{\text{silicon}}\}$, is needed for manufacturing purposes; this will be pursued in a future work along with an analysis of robustness to fabrication imperfections. That said, the final designs presented here all have significant portions which are already binary.

3.1. Coupler designs

We now present five results which suggest our method is indeed able to design arbitrary single-mode, linear nanophotonic devices. These results comprise of couplers between the following nanophotonic waveguides:

1. coupling between waveguides of different refractive index and width (Fig. 2);
2. coupling between waveguide modes of different order and symmetry (Fig. 3);
3. coupling between waveguides that confine light using different principles (index guided vs. distributed Bragg reflection guided), i.e., between a slab waveguide and a photonic crystal fiber (Fig. 4)

#161309 - $15.00 USD Received 11 Jan 2012; revised 7 Mar 2012; accepted 7 Mar 2012; published 14 Mar 2012

4. coupling from a dielectric to a plasmonic metal-insulator-metal waveguide (Fig. 5); and

5. coupling from a dielectric waveguide to a (plasmonic) metal wire (Fig. 6).

All the designs presented are both highly efficient ($\sim$ 98% coupling efficiency, in contrast to previous designs which achieve only $\sim$ 70% coupling efficiency [8, 9]) and extremely compact (with footprints of only 1.5-4 square vacuum wavelengths).

Note, however, that the small footprint of the designs presented does not imply small, unresolvable feature sizes. On the other hand, assuming a vacuum wavelength of 1550 nm, the smallest possible feature in any of the examples presented is still 37 nm $\times$ 37 nm (see Fig. 2, for example), as given by the size of a single grid point; placing virtually all designs within reach of current-generation lithographic systems.

In addition, good starting points were not required; all initial designs were simply $\varepsilon = 9$ everywhere (a somewhat arbitrary guess, other values work as well). Finally, only 15 minutes on a single-core personal computer were needed to obtain each design.

In the appendix, we further demonstrate the generality of our method by presenting several additional examples including

1. coupling between all four modes of a wide dielectric waveguide;

2. coupling from a wide, low-index waveguide to the output waveguides in Figs 3-6; and

3. coupling to selected channels of a set of five plasmonic waveguides.

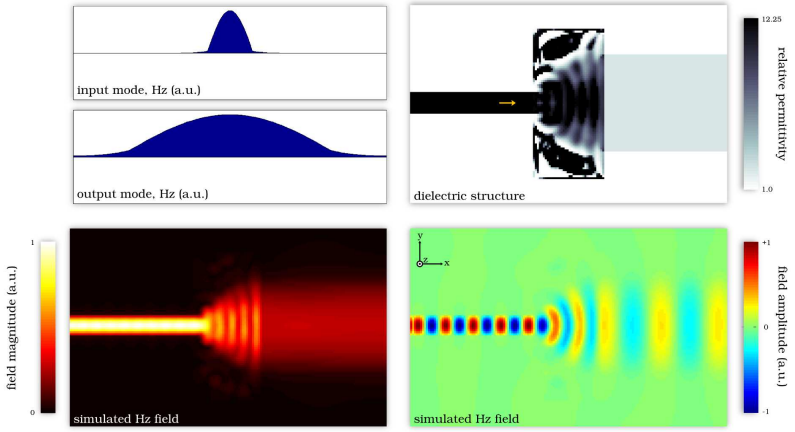

Fig. 2. Coupler from a narrow, high-index ($\varepsilon = 12.25$) waveguide to a wide, low-index ($\varepsilon = 2.25$) waveguide. The H_z^{perfect} boundary values used as the design objective are shown in the upper-left plots, the generated structure is shown in the upper-right plot, and the simulated H_z fields of the device are shown in the bottom two plots. The computed efficiency of the coupler is high, 99.8%, and the device is also extremely compact, convering only 36 $\times$ 76 grid points, where the vacuum wavelength is 42 grid points (footprint of 1.55 square vacuum wavelengths). Computation time was 15 minutes on a personal computer.

#161309 - $15.00 USD Received 11 Jan 2012; revised 7 Mar 2012; accepted 7 Mar 2012; published 14 Mar 2012

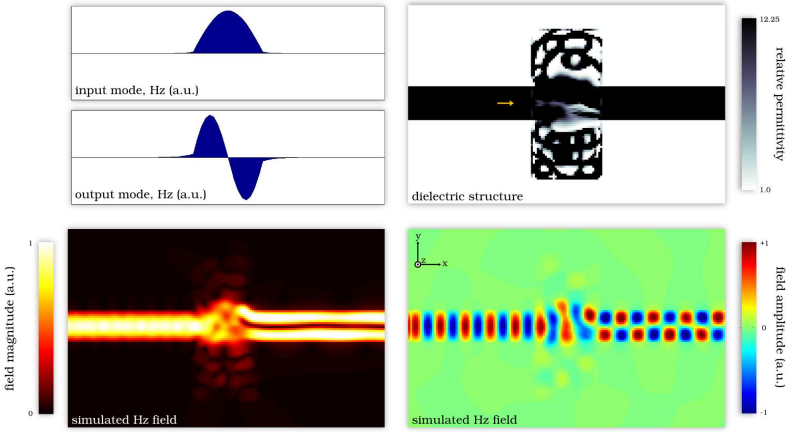

Fig. 3. Coupler that converts the fundamental waveguide mode to the second-order waveguide mode. This problem is quite difficult since the two modes are of opposite symmetry. For example, adiabatic approaches cannot be applied to this case. However, our method produces a device (which has the same dimensions and vacuum wavelength as Fig. 2) with a coupling efficiency of 98.0%. Computation time was 15 minutes on a personal computer.

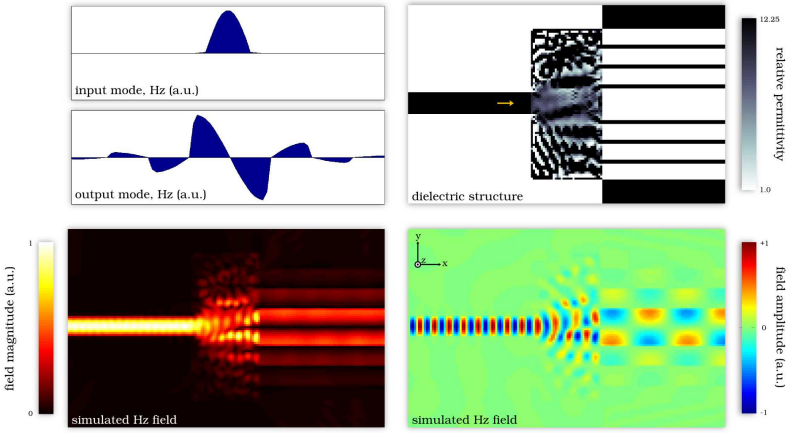

Fig. 4. Coupler between a dielectric slab waveguide to an air-core waveguide. Here, not only are the modes of opposite symmetry, but the output waveguide operates on a fundamentally different principle (distributed reflection) than the input waveguide (index guided). The device still achieves an efficiency of 98.9%, demonstrating the versatility of our method. The vacuum wavelength is 25 grid points, while the device footprint is still 36×76 grid points (footprint of 4.38 square vacuum wavelengths). Computation time was 15 minutes on a personal computer.

#161309 - $15.00 USD Received 11 Jan 2012; revised 7 Mar 2012; accepted 7 Mar 2012; published 14 Mar 2012

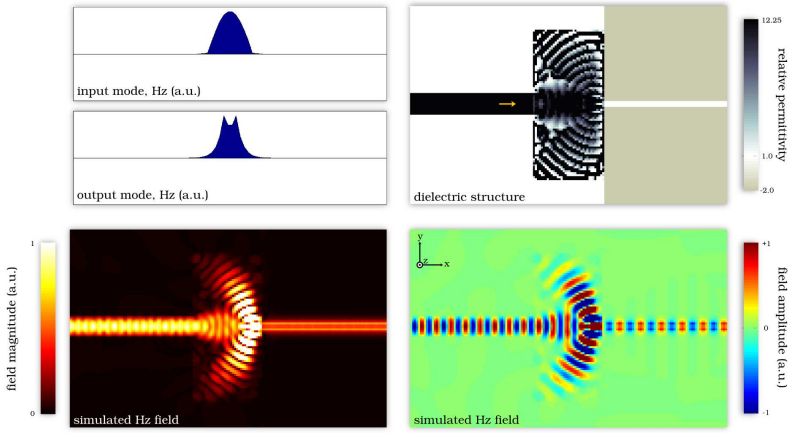

Fig. 5. Coupler between a dielectric slab waveguide to a plasmonic metal-insulator-metal waveguide. The efficiency of the device is 97.5% and has the same wavelength and footprint as the device in Fig. 4. Computation time was 15 minutes on a personal computer.

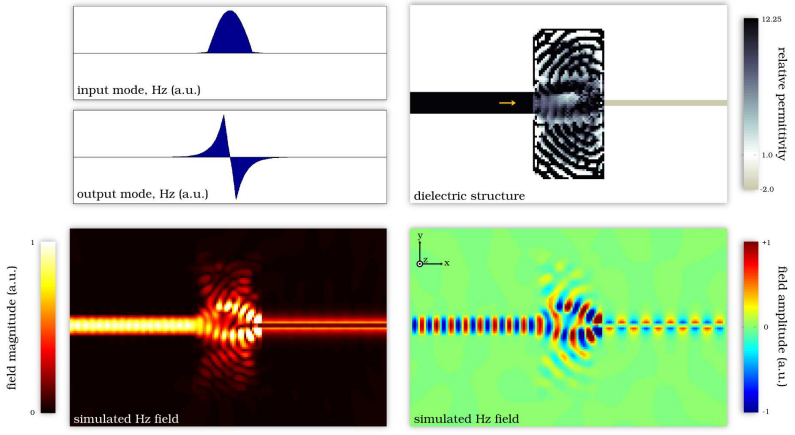

Fig. 6. Coupler between a dielectric slab waveguide to a plasmonic wire waveguide. The efficiency of the device is 99.1% and has the same wavelength and footprint as the device in Fig. 4. Computation time was 15 minutes on a personal computer.

#161309 - $15.00 USD Received 11 Jan 2012; revised 7 Mar 2012; accepted 7 Mar 2012; published 14 Mar 2012

4. Conclusion

We develop a fundamentally new approach to designing physical structures, which we term "objective-first", in that we choose to satisfy the design objective even above satisfying the physical equation which governs its operation. We then apply this approach to the design of various nanophotonic waveguide couplers, and show that our method produces high-efficiency designs ($\sim$ 98% efficiency) in small footprints (1.5-4 square vacuum wavelengths) without needing a good starting point. Furthermore, we suggest that such a methodology may be applicable to the design of any single-mode, linear nanophotonic device.

A. Appendix A

Additional mode coupler designs In this section, we present additional mode coupler designs. A wide, high-index waveguide is used at both the input and output ports, and all permutations of couplers are fabricated among the first four propagating modes [see Figs. 7–12].

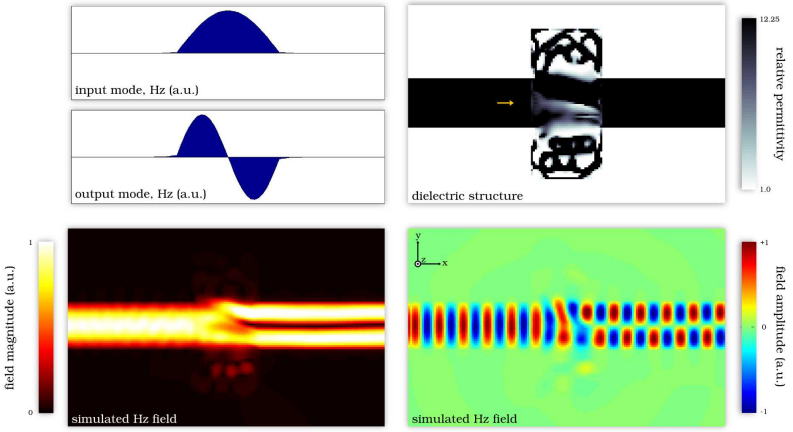

Fig. 7. Coupler from the first-order to the second-order mode of a wide dielectric waveguide. Efficiency: 99.3%, footprint: 1.55 square vacuum wavelengths.

#161309 - $15.00 USD Received 11 Jan 2012; revised 7 Mar 2012; accepted 7 Mar 2012; published 14 Mar 2012

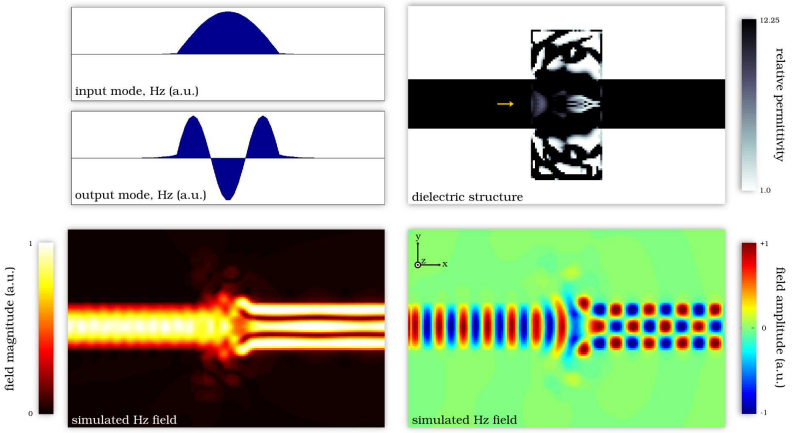

Fig. 8. Coupler from the first-order to the third-order mode of a wide dielectric waveguide. Efficiency: 98.3%, footprint: 1.55 square vacuum wavelengths.

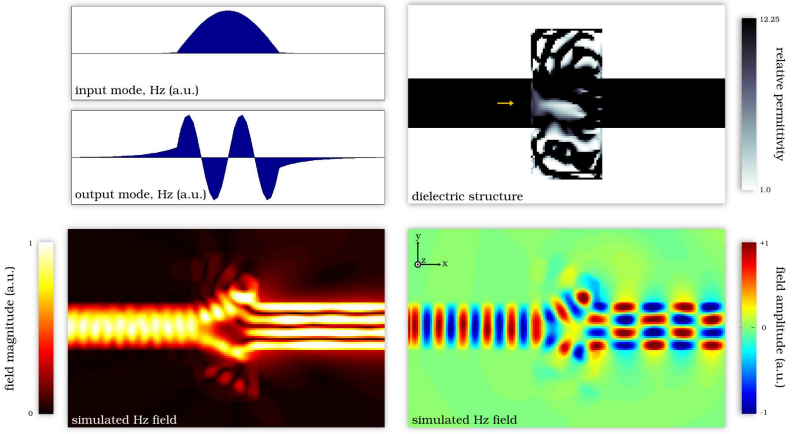

Fig. 9. Coupler from the first-order to the fourth-order mode of a wide dielectric waveguide. Efficiency: 90.6%, footprint: 1.55 square vacuum wavelengths.

#161309 - $15.00 USD Received 11 Jan 2012; revised 7 Mar 2012; accepted 7 Mar 2012; published 14 Mar 2012

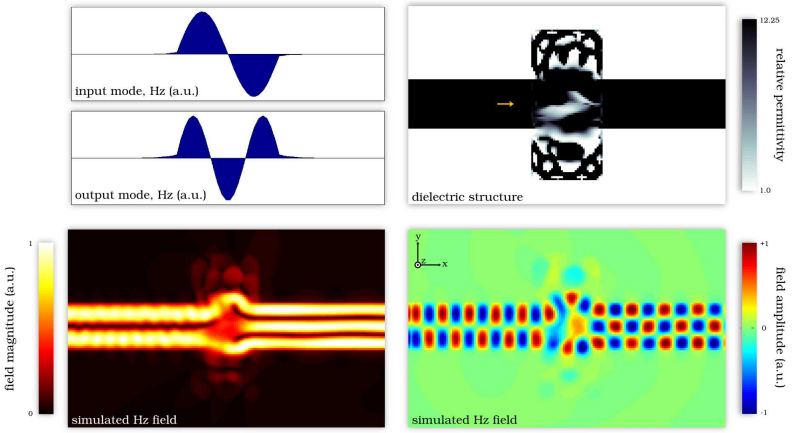

Fig. 10. Coupler from the second-order to the third-order mode of a wide dielectric waveguide. Efficiency: 96.8%, footprint: 1.55 square vacuum wavelengths.

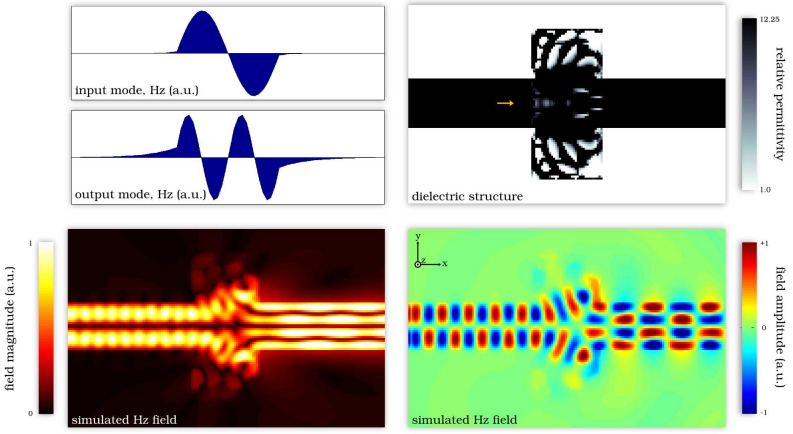

Fig. 11. Coupler from the second-order to the fourth-order mode of a wide dielectric waveguide. Efficiency: 86.3%, footprint: 1.55 square vacuum wavelengths.

#161309 - $15.00 USD Received 11 Jan 2012; revised 7 Mar 2012; accepted 7 Mar 2012; published 14 Mar 2012

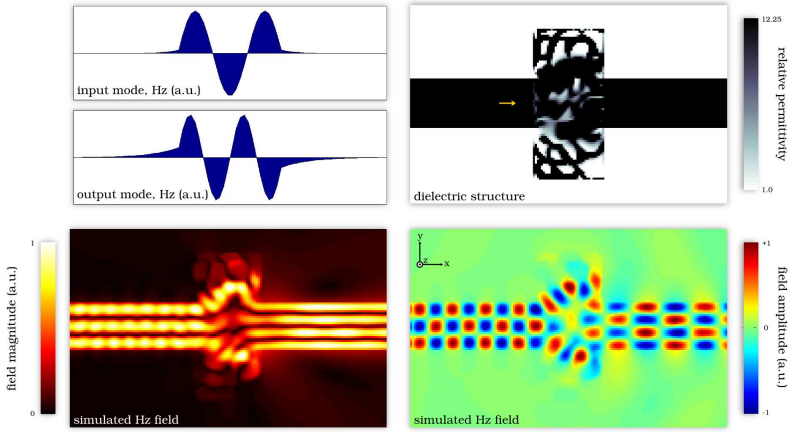

Fig. 12. Coupler from the third-order to the fourth-order mode of a wide dielectric waveguide. Efficiency: 80.1%, footprint: 1.55 square vacuum wavelengths.

#161309 - $15.00 USD Received 11 Jan 2012; revised 7 Mar 2012; accepted 7 Mar 2012; published 14 Mar 2012

B. Appendix B

Additional designs with wide, low-index input waveguide We now reproduce Figs 3-6 but instead use a wide, low-index waveguide as the input. Once again, this is to demonstrate the generality of our method; namely, that it can be applied to the design of nearly any single-mode, linear nanophotonic device [see Figs. 13–16].

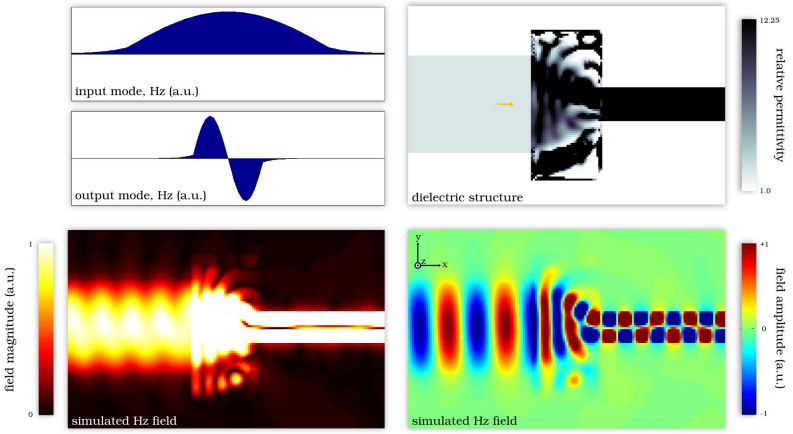

Fig. 13. Coupler from a wide, low-index waveguide to the second-order mode of a narrow, high-index waveguide. Efficiency: 96.9%, footprint: 1.55 square vacuum wavelengths.

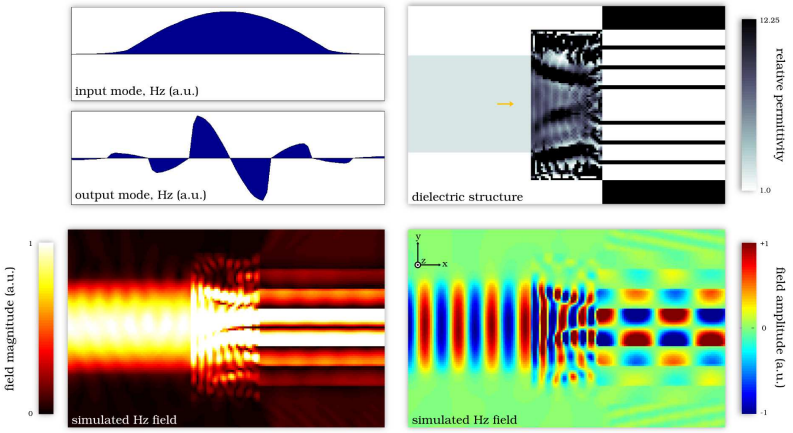

Fig. 14. Coupler from a wide, low-index waveguide to an “air-core” waveguide mode. Efficiency: 99.0%, footprint: 4.38 square vacuum wavelengths.

#161309 - $15.00 USD Received 11 Jan 2012; revised 7 Mar 2012; accepted 7 Mar 2012; published 14 Mar 2012

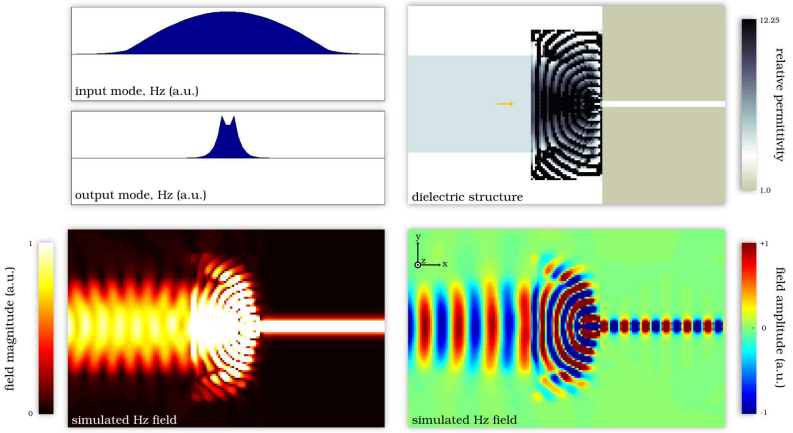

Fig. 15. Coupler from a wide, low-index waveguide to a metal-insulator-metal plasmonic waveguide mode. Efficiency: 96.7%, footprint: 4.38 square vacuum wavelengths.

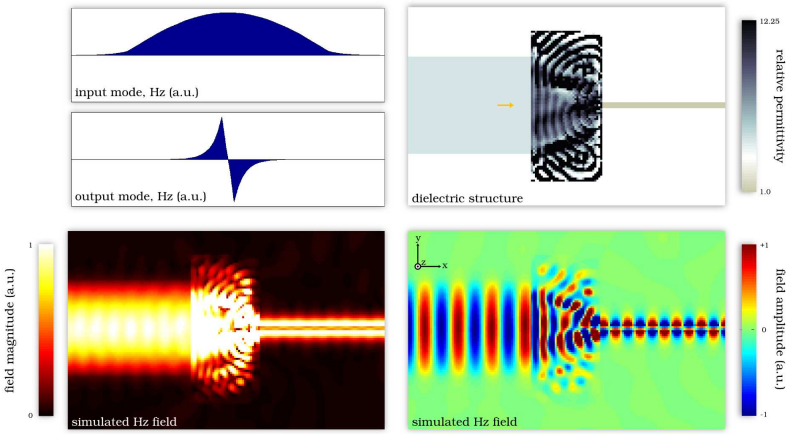

Fig. 16. Coupler from a wide, low-index waveguide to a plasmonic wire waveguide mode. Efficiency: 99.7%, footprint: 4.38 square vacuum wavelengths.

#161309 - $15.00 USD Received 11 Jan 2012; revised 7 Mar 2012; accepted 7 Mar 2012; published 14 Mar 2012

C. Appendix C

Additional designs with multiple output plasmonic waveguides We also present “selector” designs where photons are coupled to only one of five possible plasmonic output waveguides. We demonstrate these selector designs for both metal-insulator-metal and metal-wire plasmonic waveguides [see Figs. 17–22].

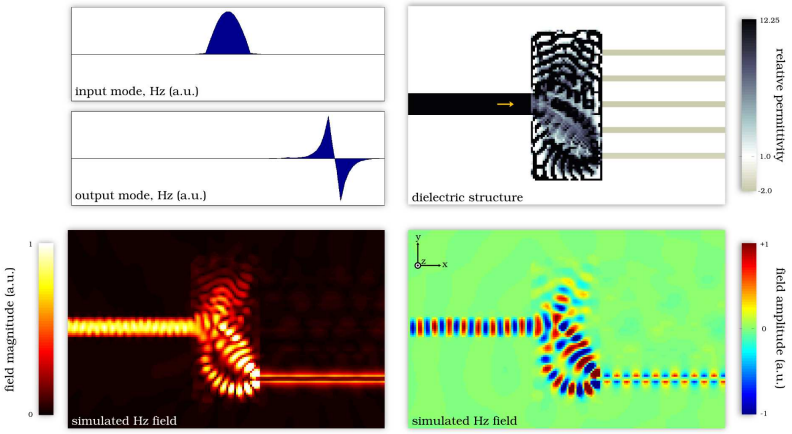

Fig. 17. Coupler from a dielectric waveguide to the lowest branch of a set of five plasmonic wire waveguides. Efficiency: 94.0%, footprint: 4.38 square vacuum wavelengths.

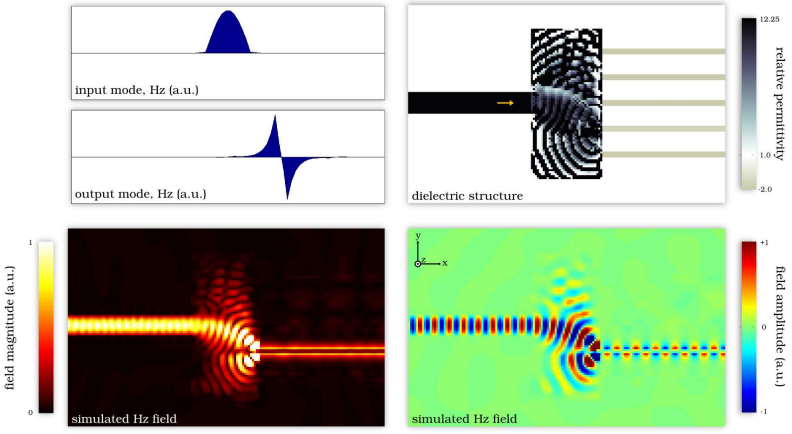

Fig. 18. Coupler from a dielectric waveguide to the second branch of a set of five plasmonic wire waveguides. Efficiency: 97.3%, footprint: 4.38 square vacuum wavelengths.

#161309 - $15.00 USD Received 11 Jan 2012; revised 7 Mar 2012; accepted 7 Mar 2012; published 14 Mar 2012

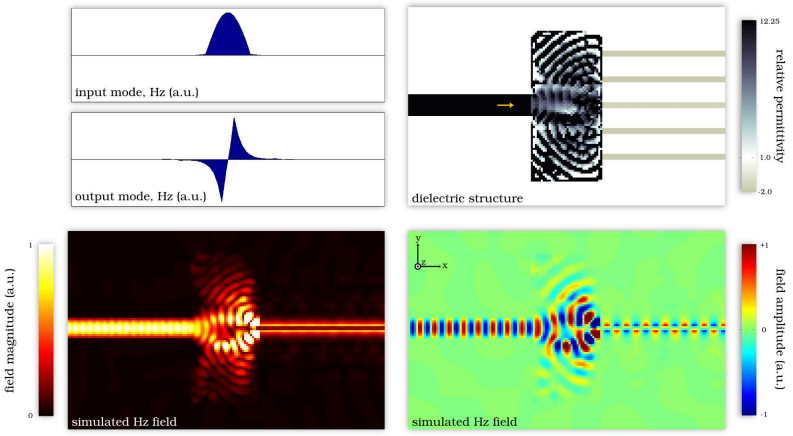

Fig. 19. Coupler from a dielectric waveguide to the middle branch of a set of five plasmonic wire waveguides. Efficiency: 98.5%, footprint: 4.38 square vacuum wavelengths.

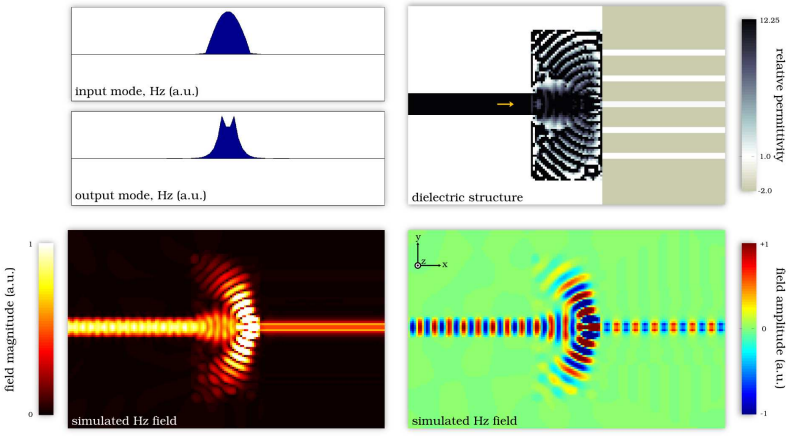

Fig. 20. Coupler from a dielectric waveguide to the middle branch of a set of five plasmonic metal-insulator-metal waveguides. Efficiency: 97.7%, footprint: 4.38 square vacuum wavelengths.

#161309 - $15.00 USD Received 11 Jan 2012; revised 7 Mar 2012; accepted 7 Mar 2012; published 14 Mar 2012

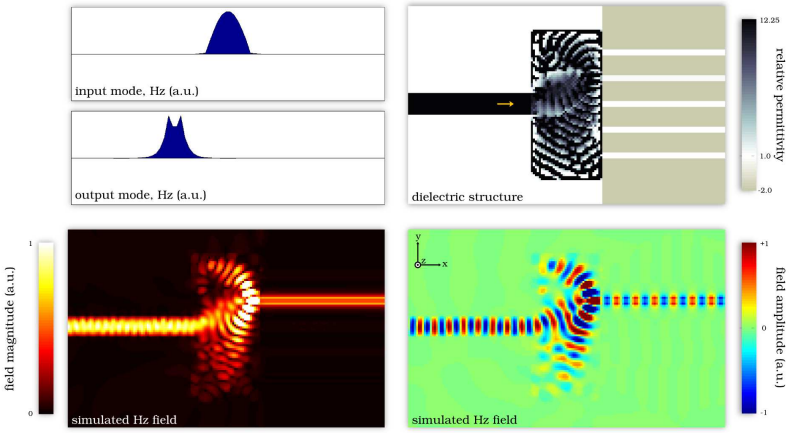

Fig. 21. Coupler from a dielectric waveguide to the fourth branch of a set of five plasmonic metal-insulator-metal waveguides. Efficiency: 95.6%, footprint: 4.38 square vacuum wavelengths.

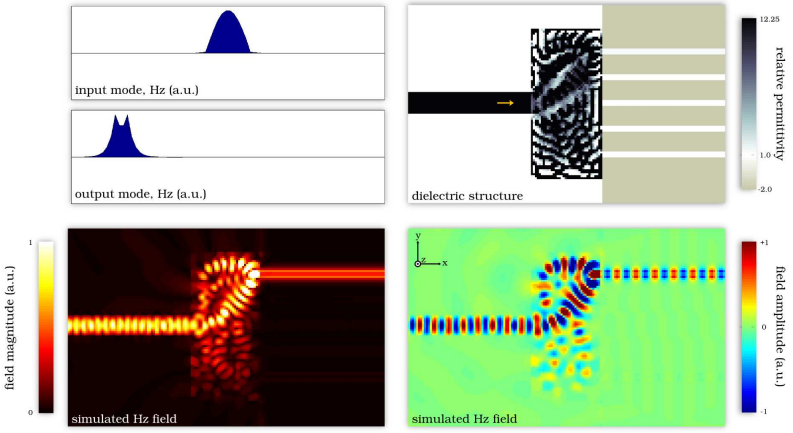

Fig. 22. Coupler from a dielectric waveguide to the uppermost branch of a set of five plasmonic metal-insulator-metal waveguides. Efficiency: 87.5%, footprint: 4.38 square vacuum wavelengths.

#161309 - $15.00 USD Received 11 Jan 2012; revised 7 Mar 2012; accepted 7 Mar 2012; published 14 Mar 2012

Acknowledgments

This work has been supported by the AFOSR MURI for Complex and Robust On-chip Nanophotonics (Dr. Gernot Pomrenke), grant number FA9550-09-1-0704. The Matlab code used is available online [10].

#161309 - $15.00 USD Received 11 Jan 2012; revised 7 Mar 2012; accepted 7 Mar 2012; published 14 Mar 2012